의학석사 학위논문

Spectral CT imaging-based quantification of iodized oil retention following chemoembolization: phantom and animal studies

화학 색전술 후 요오드화 기름 침착의 스펙트럼 CT 영상 기반 정량화 : 팬텀 및 동물 연구

2021 년 2 월

서울대학교 대학원
의학과 영상의학전공
강범식

Spectral CT imaging-based quantification of iodized oil retention following chemoembolization: phantom and animal studies

지도교수 정진욱

이 논문을 의학석사 학위논문으로 제출함

2020 년 10 월

서울대학교 대학원
의학과 영상의학전공
강범식

강범식의 석사 학위논문을 인준함

2021 년 1 월

위 원 장 이정민 (인)
부 위 원 장 정진욱 (인)
위 원 이남준 (인)

Abstract

Spectral CT imaging-based quantification of iodized oil retention following chemoembolization: phantom and animal studies

Beomsik Kang
Department of Ratdiology, College of Medicine
The Graduate School
Seoul National University

Purpose: To evaluate the accuracy of iodine quantification using spectral CT and the potential of quantitative iodized oil analysis as an imaging biomarker of chemoembolization.

Materials and Methods: A phantom of an artificial liver with six artificial tumors containing different amounts of iodized oil (0 to 8 vol%) was scanned by a spectral CT machine, and the iodized oil density (mg/mL) and Hounsfield unit (HU) values were measured. Furthermore, VX2 hepatoma was induced in 23 rabbits. After chemoembolization using iodized oil chemoemulsion, the rabbits were scanned by a spectral CT scanner. The

accumulation of iodized oil in the tumor was quantified in terms of iodized oil density and HU, and the performances in predicting a pathological complete response (CR) were evaluated by receiver operating characteristic curve analyses.

Results: The mean difference between true iodine densities and spectral image-based measurements was 0.5 mg/mL. The mean HU was highly correlated with the mean iodine density (r^2 = 1.000, p < .001). In the animal study, a pathological CR was observed in 17 out of 23 rabbits (73.9%). The area under the curve values of iodine and HU measurements ranged from .863 to .882. A tumoral iodine density of 3.57 mg/mL, which corresponds to 0.7 vol% iodized oil in the tumor, predicted a pathological CR with a sensitivity of 70.6% and a specificity of 100.0%.

Conclusion: Spectral CT imaging has a potential to predict tumor responses after chemoembolization by quantitatively assessing iodized oil in targets.

.....

keywords : transarterial chemoembolization, hepatocellular carcinoma, spectral CT, iodized oil, quantification

Student Number : 2015-22008

Contents

List of Figures

Introduction

In conventional chemoembolization, iodized oil accumulation after the procedure is regarded as an important imaging biomarker to predict tumor response and patient survival [1, 2]. However, iodized oil deposition is usually evaluated in clinical practice by a subjective visual assessment of computed tomography (CT) images. Accordingly, the Society of Interventional Radiology recommends using a five-grade system (no uptake, less than 10% uptake, 10%-50% uptake, 51%-99% uptake, and complete uptake) in reporting iodized oil retention after chemoembolization [3]. However, this subjective grading system tarnishes the value of iodized oil retention as an imaging biomarker of chemoembolization, which merits the development of quantitative imaging tools to reliably determine iodized oil accumulation.

In this regard, recent studies introduced Hounsfield unit (HU)-based quantitative methods to measure iodized oil retention after chemoembolization [4, 5]. Although iodized oil increases the CT numbers of a treated tumor, simply measuring the HU can lead to erroneous conclusions given the heterogeneous imaging texture of HCCs. HCCs may contain regional hemorrhage, fat, fibrous septa, and rarely calcification [6, 7]. Furthermore, even in cases of a homogeneous HCC, a post-chemoembolization HU is a composite result from CT values of tumor tissue and accumulated iodized oil. Moreover, iodized oil quantified as an HU cannot be translated to an actual amount (i.e., volume or density) of iodized oil in the tumor. The lack of information regarding the actual amount of iodized oil in the tumor tissue prevents a better understanding of conventional chemoembolization in relation to pre-procedural planning of iodized oil dosage, optimal embolic endpoints, etc.

Recently introduced multilayer detectors enable acquisition of spectral

imaging data with a single-source CT scan. Dual-energy information, retrospectively analyzed after a single scan, allow the differentiation and quantification of materials such as iodine and calcium at all times [8-10]. In patients with HCC, arterial enhancement of a tumor can be quantified by measuring the amount of iodinated contrast agents on pre-treatment spectral CT imaging, and the parameters have potential in predicting the survival outcome after chemoembolization [8]. On the similar principle, the iodine density of an iodized oil-laden HCC can be calculated using a post-chemoembolization spectral CT scan. By using a known iodine density in commercially-available iodized oil (i.e., 480 mg/mL), the detected iodine density (mg/mL) can be easily translated into the iodized oil volume (mL). If this process measures the amount of iodized oil in a treated tumor accurately and reproducibly, this technique may be a useful method to assess the chemoembolization effectiveness and to predict the patient prognosis.

Hence, this experimental study was conducted to evaluate the accuracy of iodine quantification using spectral CT imaging and the potential of quantitative iodized oil analysis as an imaging biomarker of chemoembolization.

Materials and Methods

Phantom preparation

The phantom for HCC in liver tissue consisted of an artificial liver and six artificial tumors labeled with iodized oil (Lipiodol; Andre Guerbet, Aulnay-Sous-Bois, France) at different concentrations. The HU values of the artificial liver and tumors were designed based on the oil/water phantom preparation method described in previous studies [11, 12]. The target CT number of the artificial liver was 60 HU [13, 14] and was produced by mixing agarose (2.0% w/v) gel with “baseline solution” consisting of distilled water, 43 mM sodium dodecyl sulfate, 43 mM sodium chloride, 3.75 mM sodium azide, and 9 mM gadoterate meglumine (Dotarem; Andre Guerbet). This mixture was stirred and cooled down in a plastic container (22 × 14 × 10 cm) mirroring the size of a human liver on axial CT images. The artificial tumors comprised of six scintillation vials (volume, 40 mL; diameter, 3 cm) with iodized oil-water volume fractions of 0%, 1%, 2%, 4%, 6%, and 8% equaling iodine densities of 0 mg/mL, 4.8 mg/mL, 9.6 mg/mL, 19.2 mg/mL, 28.8 mg/mL, and 38.4 mg/mL, respectively. The “baseline solution” was mixed with iodized oil and stirred for 2 min in beakers to prepare these pre-defined volume fractions. The six mixtures were then poured in different scintillation vials and cooled to room temperature to form solid gels. The vials were then placed into the plastic container serving as the artificial liver. This tumor-containing liver phantom was then placed in the right upper part of a water-filled plastic container (30 × 22 × 18 cm), which simulated the human body size on abdomen CT images (Fig. 1).

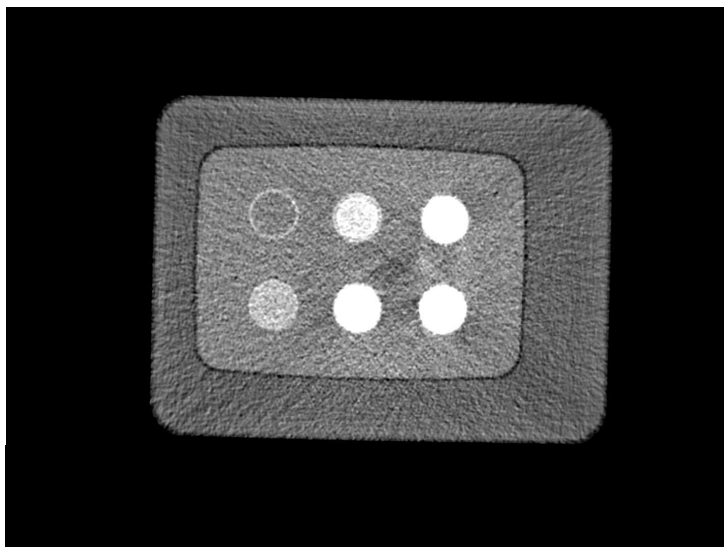

(A)

(B)

Fig. 1. Spectral CT images of the phantom containing an artificial liver and six artificial tumors with different densities of iodized oil. (A) A conventional CT image of the phantom. (B) A color-coded iodine map of the phantom.

Phantom image acquisition and analysis

The phantom was scanned by a spectral CT device (IQon Spectral CT; Philips Healthcare, Best, Netherland) with the following parameters: peak voltage = 120 kVp, automatic tube current modulation, field of view = 400 × 400 mm, and matrix = 512 × 512. The raw data were reconstructed with slice thicknesses of 1 mm and 3 mm to retrieve two image sets. In the 1 mm-reconstructed image, one author selected three consecutive image slices in the middle of the phantom and drew circular regions of interest (ROIs) to measure HU and iodine density values. These ROIs were fully placed into the artificial tumor areas. Another author analyzed the 3 mm-reconstructed images using the same method. Therefore, a total of six measurements were performed per artificial tumor.

Animal model

The animal experiment was approved by the Institutional Animal Care and Use Committee and performed in accordance with the institutional guidelines. Twenty-four male New Zealand White rabbits weighing 2.8 to 3.3 kg and VX2 carcinoma maintained by successive transplantations of tumor cells in carrier rabbits were used in this experiment. Anesthesia was induced by injecting zolazepam (5 mg/kg, Zoletil; Virbac, Carros Cedex, France) and xylazine (10 mL/kg, Rompun; Bayer-Schering Pharma, Berlin, Germany) in the hind limb. After an abdominal midline incision, a 1 mm-sized, cubic tumor block was implanted into the liver. Hemostasis was achieved by applying gentle pressure with cotton swabs. Tumor growth was identified on a 3-phase dynamic CT scan (IQon Spectral CT; Philips Healthcare) 20 days after VX2 carcinoma tissue implantation (Fig. 2.). After the acquisition of unenhanced CT images, 10 mL of contrast medium (iopromide; Ultravist 370; Schering, Berlin, Germany) was administered at a

flow rate of 0.5 mL/s through the auricular vein. Using a bolus-tracking technique, the arterial and portal phase scans were conducted 7 and 23 seconds after descending thoracic aorta enhancement to 80 HU, respectively. Individual tumor sizes were measured as the longest diameter on axial CT images of the arterial phase scan. During the whole experiment, the rabbits were raised in individual conventional cages with 12-hour light per day and rabbit pellets containing carbohydrate, protein, fat, and dietary fibers.

Chemoembolization

Chemoembolization was performed using iodized oil emulsion by an interventional radiologist (13 years of experience in interventional radiology) one day after the pre-chemoembolization CT scan. After anesthesia with the same method used in tumor modeling, an 18-gauge angiocatheter was inserted into the right auricular artery of the rabbit. Through the arterial access, a 1.7-Fr microcatheter (Progreat lambda; Terumo, Tokyo, Japan) and a 0.016-inch guidewire (Meister, Asahi Intecc, Nagoya, Japan) were introduced to the proper hepatic artery under fluoroscopic guidance [2]. Doxorubicin hydrochloride powders were blended with contrast media at the concentration of 20 mg/mL. Iodized oil was mixed with the doxorubicin hydrochloride solution at a 4:1 volume ratio [15] using a three-way stopcock pumping method, and 0.2 mL of the chemoemulsion (0.08 mg of doxorubicin hydrochloride) was infused through the microcatheter into each rabbit.

(A)

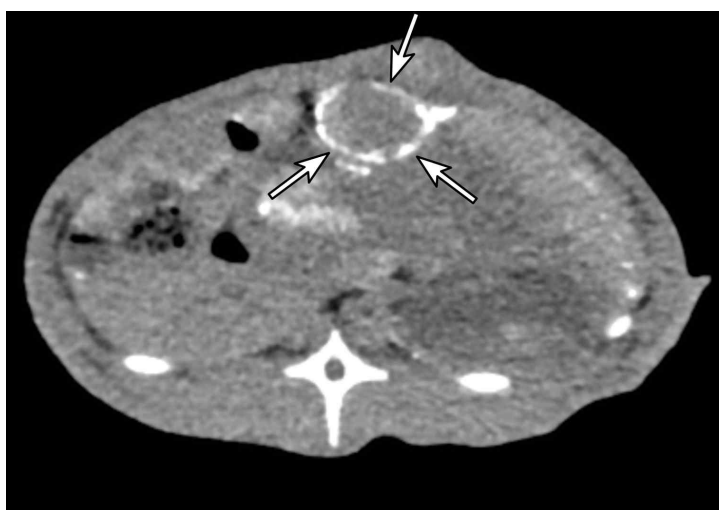

(B)

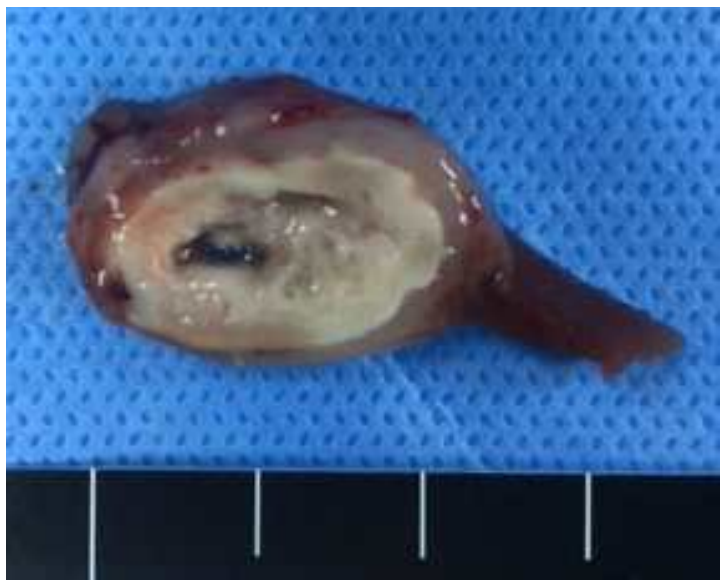

(C)

(D)

Fig. 2. An example of rabbit VX2 tumor model determined to pathological CR.

(A) An axial image of the pre-chemoembolization CT scan in a rabbit demonstrates a VX2 tumor (arrows) with a diameter of 2.0

cm in the liver.

(B) An axial image of the post-chemoembolization CT scan show iodized oil uptake in peripheral portion of the tumor (elliptic HU, 101.8 ± 71.4; elliptic iodine density, 2.06 ± 1.8; doughnut shape HU, 159.5 ± 75.5; doughnut shape iodine density, 3.47 ± 2.1).

(C) An axial gross specimen shows the peripherally located treated tumor with central necrosis.

(A) A hematoxylin-and-eosin stained slide demonstrates no viable cells in the treated tumor.

Spectral CT imaging and analysis

The rabbits were moved to a CT room immediately after chemoembolization and scanned by a spectral CT scanner (IQon Spectral CT; Philips Healthcare) without intravenous contrast agents using the following parameters: peak voltage = 100 kVp; automatic tube current modulation; field of view = 177 × 177 mm, matrix = 1,020 × 512, slice thickness = 1 mm. The spectral data were transferred to a dedicated workstation and analyzed using the IntelliSpace Portal software (Philips Healthcare). Because VX2 hepatoma is highly necrotic [16], two types of ROIs were placed into each tumor area. In the conventional HU mode, an axial image slice showing the largest section of a tumor was selected for each rabbit. An elliptic ROI was drawn to encompass the entire tumor. In addition, a doughnut-shaped ROI was manually drawn using the "spline" function to contain only viable tumor portions (Fig. 2). With reference to the pre-chemoembolization CT images, the central necrosis was excluded from the doughnut-shaped ROI. After measuring the ROI-based mean HU values and volumes (mL), the ROIs were transferred to iodine density maps to calculate the mean iodine density (mg/mL). Two authors conducted these imaging analyses independently, and the mean values were used for further analyses.

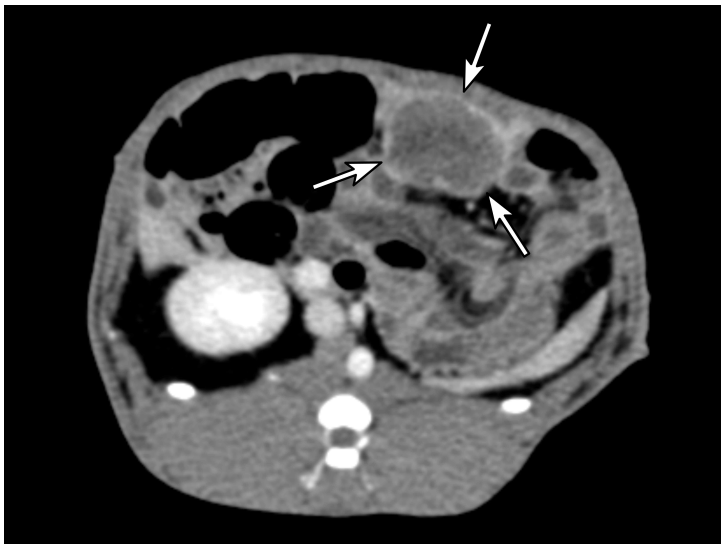

(A)

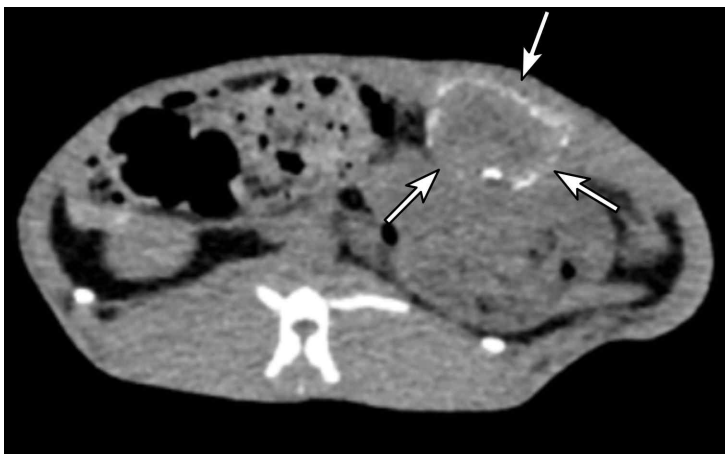

(B)

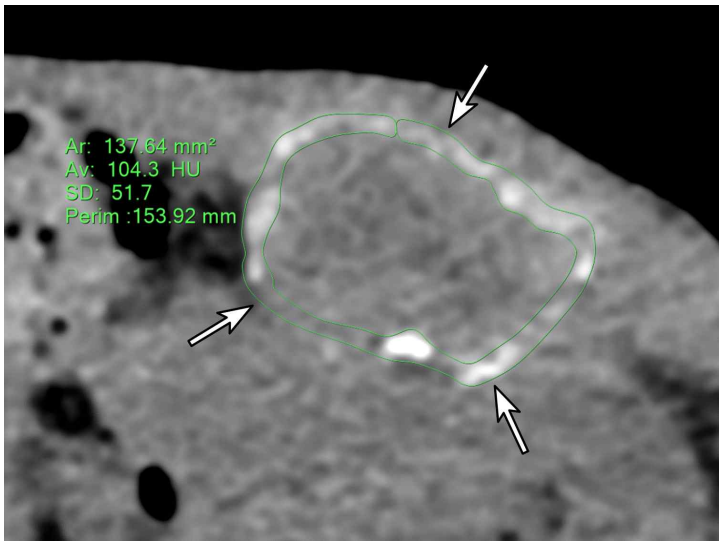

(C)

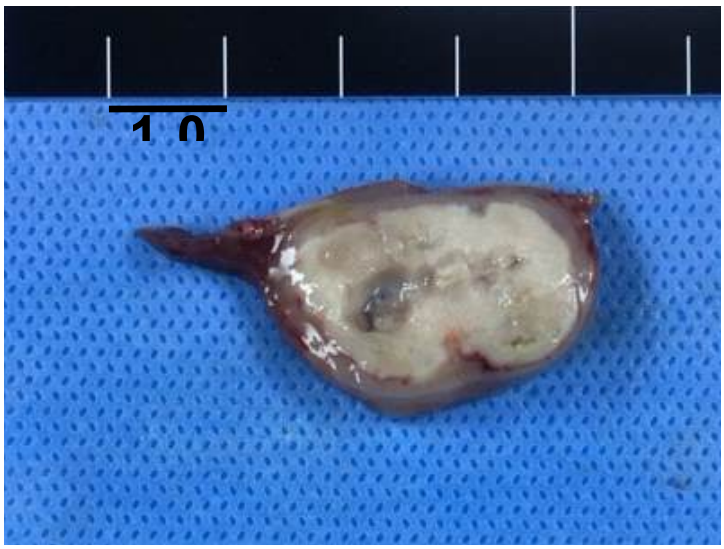

(D)

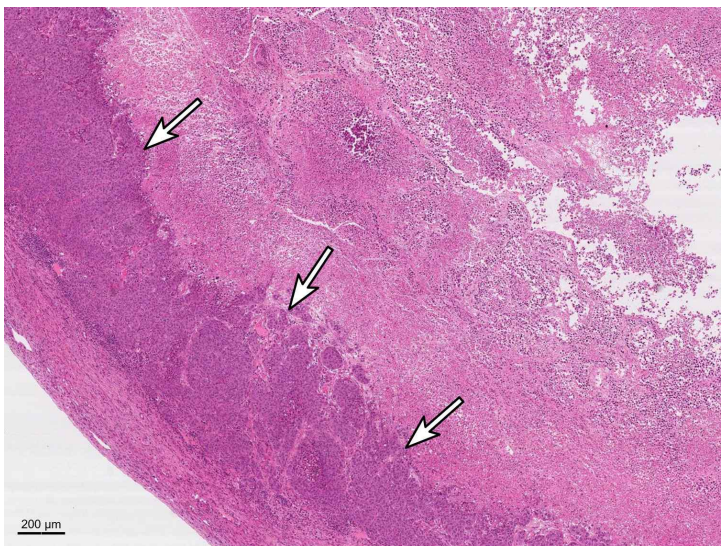

(E)

Fig. 3. An example showing the doughnut-shaped ROI analysis in a VX2 tumor model without pathological CR.

(A) An axial image of the pre-chemoembolization CT scan in a rabbit demonstrates a VX2 tumor (arrows) with a diameter of 2.6 cm in the liver.

(B) An axial image of the post-chemoembolization CT scan demonstrates iodized oil uptake in peripheral portion of the tumor (elliptic HU, 62.8 ± 39.2; elliptic iodine density, 0.84 ± 0.9; doughnut shape HU, 104.3 ± 51.7; doughnut shape iodine density, 1.68 ± 1.4).

(C) A doughnut-shaped ROI (arrows) was manually drawn on a magnified post-chemoembolization CT image to outline the viable portions of the tumor.

(D) A gross specimen of the treated tumor shows central necrosis and peripheral viable cells.

(E) A hematoxylin-and-eosin stained slide demonstrates viable tumor cells (arrows) in the periphery of the treated tumor.

Pathological evaluation

The rabbits were euthanized with an intravenous injection of a lethal dose (7-10 mL) of xylazine hydrochloride under deep anesthesia at 7 days after the chemoembolization [15]. After laparotomy, the tumor and adjacent liver were excised en-bloc and the tissues were sectioned in the same transvers plane used for CT with a 5 mm thickness. The specimens were fixed with 10% formalin, sliced at a thickness of 5 μm in a plane similar to that of the axial CT images, and stained with the hematoxylin-and-eosin technique. One author (9 years of experience in animal research), who was blinded to the spectral CT images, selected the slice covering the largest tumor dimension and judged the pathological complete response (CR) of the tumor.

Statistical analysis

In the phantom study, a Bland-Altman plot was created to determine the accuracy of the iodine quantification using spectral CT data. The mean value of six measurements per artificial tumor was calculated, and an HU-to-iodine density conversion model was established by linear regression analysis. In the animal study, the performances of HU and iodine measurements in predicting the pathological CR were evaluated by receiver operating characteristic (ROC) curve analyses. Four ROC curves, from the elliptic HU, doughnut-shaped HU, elliptic iodine, and doughnut-shaped iodine ROIs, were compared using the method by DeLong et al. [17].

A two-sided *p*-value of less than .05 was considered to indicate a significant difference, and all statistical analyses were performed using commercially available software (MedCalc, version 18.11.3; MedCalc Software, Ostend, Belgium).

Calculation of the therapeutic chemoemulsion dose

From the result of the doughnut-shaped iodine ROI analysis, a cut-off value to predict the pathological CR was determined using the Youden's index. Based on the known iodine density in iodized oil (480 mg/mL), the cut-off value was converted to a volume percentage (vol%) of iodized oil in a tumor. In addition, a therapeutic dose of iodized oil chemoemulsion was calculated for a rabbit containing a VX2 tumor. The tumor size was determined as the mean value of all VX2 tumors tested in the present study, and viable tumor cells were assumed to be present peripherally at a 2-mm thickness. According to the literature describing the VX2 hepatoma model [18], the viable portion of a VX2 tumor has an approximately two times higher blood volume and a three times higher arterial enhancement fraction, compared to the same volume of a normal liver. Therefore, this study assumed that chemoemulsion infused at the proper hepatic artery is accumulated in the viable portion of a VX2 tumor six times higher than the same volume of a normal liver [8, 19]. Hence, the required iodine and iodized oil amounts to achieve a pathological CR were calculated as follow:

$$Tumor\ iodine\,(mg) = iodine\ cut-off\,(mg/mL) \times viable\ tumor\ volume\,(mL)$$

$$Liver\ iodine\,(mg) = \frac{iodine\ cut-off\,(mg/mL)}{6} \times liver\ volume\,(mL)$$

$$Total\ iodine\,(mg) = tumor\ iodine\,(mg) + liver\ iodine\,(mg)$$

$$Total\ iodized\ oil\ (mL) = total\ iodine\ (mg) \div 480\ (mg/mL)$$

Based on the previous literature [20], the liver volume of a 3.0-kg rabbit containing a VX2 tumor was established as 86 mL. Since the iodized oil chemoemulsion was a mixture of iodized oil and doxorubicin hydrochloride at a 4:1 volume ratio, the total amount of chemoemulsion required was calculated as follows:

$$Total\ chemoemulsion\ (mL) = \frac{5}{4} \times total\ iodized\ oil\ (mL)$$

It was assumed that tumor and liver vascularity are the only factors affecting the chemoemulsion distribution, and the chemoemulsion was regarded as evenly distributed in the tumor. Other variables such as intratumoral heterogeneity and iodized oil washout were not considered in our simulation.

Results

Phantom study

The mean difference between true iodine densities and spectral image-based measurements was 0.5 mg/mL (Fig. 3). The lower and upper limits (± 1.96 standard deviation [SD]) were -2.6 mg/mL and 1.6 mg/mL, respectively. The discrepancy was relatively noticeable in the high-density lesion (8 vol%, 38.4 mg/mL), but the largest difference between a single measurement and its true value was only 2.1 mg/mL. The mean HU was highly correlated with the mean iodine density (r^2 = 1.000, p < .001). Within the tested range of iodine densities, HU values could be converted into the corresponding iodine densities using the following equation (Fig. 4):

$$Iodine\ density\ \left(\frac{mg}{mL}\right) = 0.0479 \times HU - 1.480$$

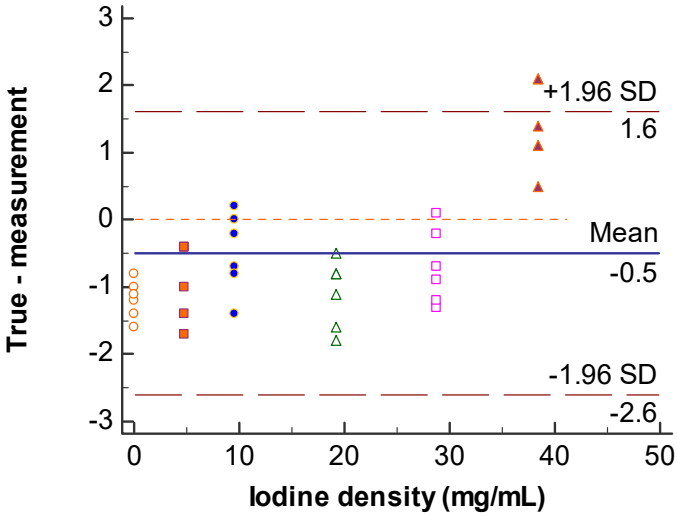

Fig 4. A Bland-Altman plot showing the difference between true iodine densities and spectral CT-based measurement values.

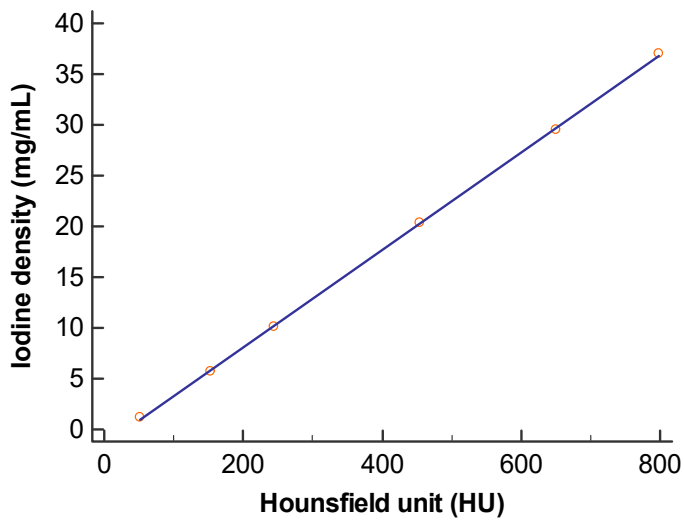

Fig 5. A scatter diagram with the regression line presenting the correlation between iodine density and HU on spectral CT images.

Animal study

The VX2 tumor was successfully induced in 23 out of 24 rabbits, and the rabbit with failed tumor induction was excluded from further analyses. The tumor sizes ranged from 1.6 cm to 3.2 cm with a mean value of 2.4 cm (SD, 0.4 cm). A pathological CR was observed in 17 out of 23 rabbits (73.9%). In the ROC curve analyses for predicting a pathological CR, the area under the curve values of elliptic HU, doughnut-shaped HU, elliptic iodine, and doughnut-shaped iodine measurements were .882 (95% confidence interval [CI], .680 to .978), .863 (95% CI, .656 to .969), .873 (95% CI, .668 to .974), and .863 (95% CI, .656 to .969), respectively (Fig. 5). There was no significant difference among the four methods.

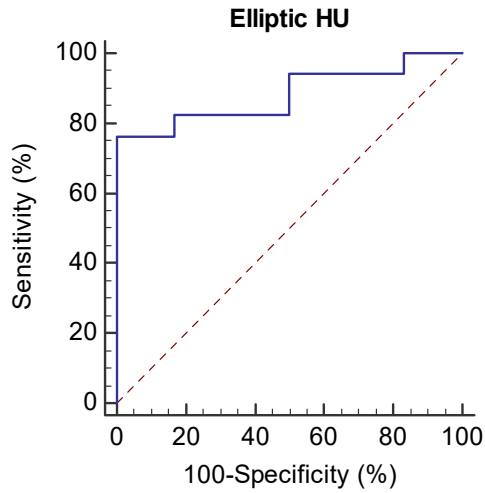
Elliptic HU
Sensitivity (%)
100
80
60
40
20
0
0
20
40
60
80
100
100-Specificity (%)

(A)

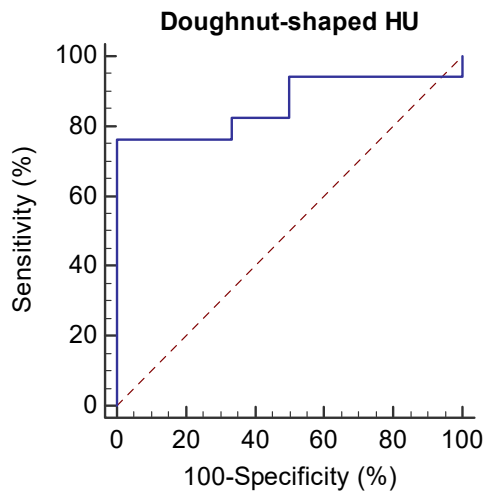
Doughnut-shaped HU
Sensitivity (%)
100
80
60
40
20
0
0
20
40
60
80
100
100-Specificity (%)

(B)

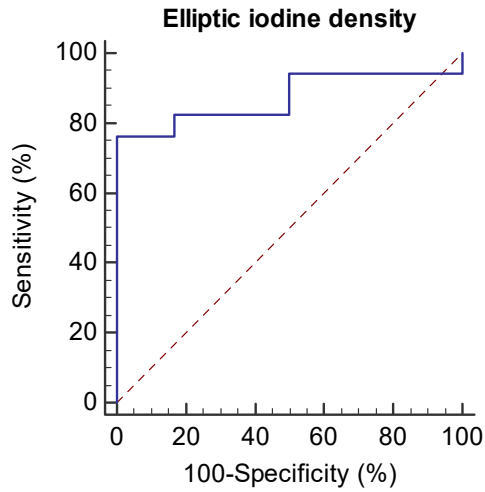

(C)

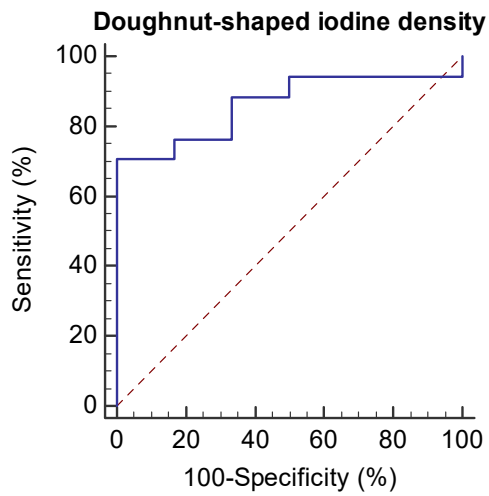

(D)

Fig. 6. The ROC curves of iodized oil quantification predicting a pathological CR after chemoembolization.

(A) HU measurement using an elliptic ROI (area under the curve

values [AUC], .882; 95% confidence interval, .680 to .978).

(B) HU measurement using a doughnut-shaped ROI (AUC, .863; 95% confidence interval, .656 to .969).

(C) Iodine density (mg/mL) measurement using an elliptic ROI (AUC, .873; 95% confidence interval, .668 to .974).

(D) Iodine density (mg/mL) measurement using a doughnut-shaped ROI (AUC, .863; 95% confidence interval, .656 to .969).

Calculation of the therapeutic chemoemulsion dose

The cut-off value for iodine density in the doughnut-shaped iodine ROI analysis was 3.57 mg/mL, which corresponds to a 0.7 vol% of a tumor. This cut-off value yielded a sensitivity of 70.6% and a specificity of 100.0% in predicting a pathological CR. Assuming that a VX2 tumor is 2.4 cm in diameter and viable tumor cells are located at its border with a 2-mm thickness, the viable tumor volume is calculated as 3.05 mL. Therefore, 62.5 mg of iodine (10.9 mg and 51.6 mg for the tumor and liver, respectively) is needed to achieve a pathological CR, which corresponds to 0.13 mL of iodized oil. Given that the volume ratio of iodized oil and doxorubicin solution is 4:1, 0.16 mL of chemoemulsion was associated with a pathological CR.

Discussion

In clinical practice, the initial CR after chemoembolization is one of the most important prognostic factors in patients with HCC [21]. A quantitative analysis of iodized oil retention can provide a reliable result that facilitates an immediate assessment of the tumor response and enables a faster treatment conversion to other interventions such as additional ablation or sorafenib administration.

There is no consensus in determining the optimal chemoemulsion dose. This is one of the crucial reasons to hinder standardization of chemoembolization worldwide. This problem is also related to determine the optimal embolic endpoint. Particularly in small- and medium-sized HCC, it is regarded as an ideal endpoint when the chemoemulsion fills the peritumoral portal veins as well as the tumor vascular bed [22]. However, the peritumoral portogram is a transient phenomenon during chemoembolization, as the chemoemulsion in the portal vein is washed out as time passes, and identification of the portal vein staining is subjective. In this context, a simulated dose of chemoemulsion may provide additional guidance to determine the endpoint of the chemoembolization. A simulation-based target dose of chemoemulsion may be set prior to the procedure, and post-procedural spectral CT imaging can be used to determine the technical completeness of chemoembolization.

In the phantom study, conventional HU values have an almost perfect linear correlation with the iodine density measured by the spectral data. At present, spectral CT scanners have very limited availability, and dual-energy CT machines require a special scan protocol and additional radiation to quantify the iodine deposition. However, using the conversion equation presented in this study, the amount of iodized oil accumulated in a tumor may be approximated with conventional CT scanners. In addition, recent

studies demonstrate that HU values between C-arm and diagnostic CT images are highly correlated [23], suggesting that the intratumoral retention of iodized oil can also be indirectly measured by a C-arm CT scan during chemoembolization procedures.

The VX2 hepatoma is an animal tumor model widely used in the translational research of chemoembolization [24, 25]. Although this is a well-established model, special cautions are required when translating the animal experiment results into changes in clinical practice. While VX2 hematoma consistently form masses with central necrosis and peripheral viable cells, human HCCs have diverse histological and radiological features [6]. Therefore, chemoembolization of human HCC frequently results in very high uptake of iodized oil in one part of the tumor and a scant uptake in another part, but the mean value cannot reflect this phenomenon appropriately. The heterogeneous nature of HCC calls for new quantifiable parameters that take into account regional discrepancies as well as the total uptake of iodized oil. Moreover, the heterogeneous uptake of iodized oil is known as one of the risk factors for local recurrence in patients treated with chemoembolization. However, the heterogeneity and defects of iodized oil uptake were not analyzed in this study, and this is one of the limitations in this study. In addition, chemoembolization is mainly applied to patients with multiple HCCs [26, 27]. Further investigations are warranted to apply the individual tumor-based analysis of the present study in a clinical context. The presented technique is also not applicable to chemoembolization using radiolucent drug-eluting microspheres. Radiopaque drug-eluting microspheres, on the other hand, contain iodine or iodine derivatives that can be measured using spectral CT images. Given that imageable microspheres have an excellent spatial match among the distributions of iodine, drug, and embolic agents [25], spectral CT imaging enables the assessment of both drug

delivery and embolization effects at a time, which may facilitate precise prognostication.

There are some limitations in the present study. Tumors were manually segmented using two-dimensional imaging data. Three-dimensional analyses of imaging data and pathological specimens can more accurately evaluate the performance of iodized oil quantification in predicting tumor responses. This method can assess the distribution of chemoemulsion in liver and tumor, and calculate the required amount of chemoemulsion more accurately than the equation based on the assumptions presented in this study. In this study, analysis of the rate of tumor necrosis was not perfromedhe three-dimensional analyses of pathological specimens can also evaluate the rate of tumor necrosis and its association with iodized oil density of tumor. In addition, the manual ROI method hampers the reproducibility in tumor segmentation. Emerging technologies such as artificial intelligence-based 3D segmentation may be combined with iodized oil quantification to provide more reproducible and accurate results. The present study utilized only an iodized oil chemoemulsion to treat rabbits, whereas gelatin sponge particle or polyvinyl alcohol particle embolization is commonly added to chemoemulsion in patients. Iodized oil quantification does not take into account the effects of additional embolization particles, and this may influence the reliability of the iodine quantification in predicting the tumor response. In the pathological evaluation, pathological CR was not determined by pathologist, and this is one of limitations in our study. In addition, the specimens were sliced in the axial plane and slides showing the largest dimension were selected to compare with corresponding spectral CT images. Although this is a commonly used method in radiology-pathology correlation studies, there may be a mismatch between the selected images and pathology slides.

Spectral CT imaging has a potential to predict tumor responses after chemoembolization by quantitatively assessing iodized oil in targets.

References

[1] Takayasu K, Muramatsu Y, Maeda T, et al. Targeted transarterial oily chemoembolization for small foci of hepatocellular carcinoma using a unified helical CT and angiography system: analysis of factors affecting local recurrence and survival rates. AJR Am J Roentgenol 2001; 176:681-8.

[2] Shim JH, Han S, Shin YM, et al. Optimal measurement modality and method for evaluation of responses to transarterial chemoembolization of hepatocellular carcinoma based on enhancement criteria. J Vasc Interv Radiol 2013; 24:316-25.

[3] Gaba RC, Lewandowski RJ, Hickey R, et al. Transcatheter Therapy for Hepatic Malignancy: Standardization of Terminology and Reporting Criteria. J Vasc Interv Radiol 2016; 27:457-73.

[4] Chen R, Geschwind JF, Wang Z, Tacher V, Lin M. Quantitative assessment of lipiodol deposition after chemoembolization: comparison between cone-beam CT and multidetector CT. J Vasc Interv Radiol 2013; 24:1837-44.

[5] Wang Z, Chen R, Duran R, et al. Intraprocedural 3D Quantification of Lipiodol Deposition on Cone-Beam CT Predicts Tumor Response After Transarterial Chemoembolization in Patients with Hepatocellular Carcinoma. Cardiovasc Intervent Radiol 2015; 38:1548-56.

[6] Choi JY, Lee JM, Sirlin CB. CT and MR imaging diagnosis and staging of hepatocellular carcinoma: part I. Development, growth, and spread: key pathologic and imaging aspects. Radiology 2014; 272:635-54.

[7] Ichikawa T, Federle MP, Grazioli L, Madariaga J, Nalesnik M, Marsh W. Fibrolamellar hepatocellular carcinoma: imaging and pathologic findings in 31 recent cases. Radiology 1999; 213:352-61.

[8] Wang J, Shen JL. Spectral CT in evaluating the therapeutic effect of transarterial chemoembolization for hepatocellular carcinoma: A retrospective study. Medicine (Baltimore) 2017; 96:e9236.

[9] McCollough CH, Leng S, Yu L, Fletcher JG. Dual- and Multi-Energy CT: Principles, Technical Approaches, and Clinical Applications. Radiology 2015; 276:637-53.

[10] Ozguner O, Dhanantwari A, Halliburton S, Wen G, Utrup S, Jordan D. Objective image characterization of a spectral CT scanner with dual-layer detector. Phys Med Biol 2018; 63:025027.

[11] Hines CD, Yu H, Shimakawa A, McKenzie CA, Brittain JH, Reeder SB. T1 independent, T2* corrected MRI with accurate spectral modeling for quantification of fat: validation in a fat-water-SPIO phantom. J Magn Reson Imaging 2009; 30:1215-22.

[12] Yin X, Guo Y, Li W, et al. Chemical shift MR imaging methods for the quantification of transcatheter lipiodol delivery to the liver: preclinical feasibility studies in a rodent model. Radiology 2012; 263:714-22.

[13] Zhang LJ, Peng J, Wu SY, et al. Liver virtual non-enhanced CT with dual-source, dual-energy CT: a preliminary study. Eur Radiol 2010; 20:2257-64.

[14] Levitt RG, Sagel SS, Stanley RJ, Jost RG. Accuracy of computed tomography of the liver and biliary tract. Radiology 1977; 124:123-8.

[15] Choi JW, Cho HJ, Park JH, et al. Comparison of drug release and pharmacokinetics after transarterial chemoembolization using diverse lipiodol emulsions and drug-eluting beads. PLoS One 2014; 9:e115898.

[16] Pascale F, Ghegediban SH, Bonneau M, et al. Modified model of VX2 tumor overexpressing vascular endothelial growth factor. J Vasc Interv

Radiol 2012; 23:809-17 e2.

[17] DeLong ER, DeLong DM, Clarke-Pearson DL. Comparing the areas under two or more correlated receiver operating characteristic curves: a nonparametric approach. Biometrics 1988; 44:837-45.

[18] Kim KW, Lee JM, Kim JH, et al. CT color mapping of the arterial enhancement fraction of VX2 carcinoma implanted in rabbit liver: comparison with perfusion CT. AJR Am J Roentgenol 2011; 196:102-8.

[19] Yang L, Zhang XM, Zhou XP, et al. Correlation between tumor perfusion and lipiodol deposition in hepatocellular carcinoma after transarterial chemoembolization. J Vasc Interv Radiol 2010; 21:1841-6.

[20] Paramo M, Garcia-Barquin P, Santa Maria E, et al. Evaluation of the rabbit liver by direct portography and contrast-enhanced computed tomography: anatomical variations of the portal system and hepatic volume quantification. Eur Radiol Exp 2017; 1:7.

[21] Kim BK, Kim SU, Kim KA, et al. Complete response at first chemoembolization is still the most robust predictor for favorable outcome in hepatocellular carcinoma. J Hepatol 2015; 62:1304-10.

[22] Miyayama S, Matsui O, Yamashiro M, et al. Ultraselective transcatheter arterial chemoembolization with a 2-f tip microcatheter for small hepatocellular carcinomas: relationship between local tumor recurrence and visualization of the portal vein with iodized oil. J Vasc Interv Radiol 2007; 18:365-76.

[23] Ishikawa T, Abe S, Hoshii A, et al. Cone-Beam Computed Tomography Correlates with Conventional Helical Computed Tomography in Evaluation of Lipiodol Accumulation in HCC after Chemoembolization. PLoS One 2016; 11:e0145546.

[24] Kim HC, Chung JW, Choi SH, et al. Augmentation of chemotherapeutic infusion effect by TSU-68, an oral targeted antiangiogenic agent, in a rabbit VX2 liver tumor model. Cardiovasc Intervent Radiol 2012; 35:168-75.

[25] Mikhail AS, Pritchard WF, Negussie AH, et al. Mapping Drug Dose Distribution on CT Images Following Transarterial Chemoembolization with Radiopaque Drug-Eluting Beads in a Rabbit Tumor Model. Radiology 2018; 289:396-404.

[26] European Association for the Study of the Liver. Electronic address eee, European Association for the Study of the L. EASL Clinical Practice Guidelines: Management of hepatocellular carcinoma. J Hepatol 2018; 69:182-236.

[27] Heimbach JK, Kulik LM, Finn RS, et al. AASLD guidelines for the treatment of hepatocellular carcinoma. Hepatology 2018; 67:358-80.

요약(국문 초록)

화학 색전술 후 요오드화 기름 침착의 스펙트럼 CT 영상 기반 정량화 : 팬텀 및 동물 연구

목적 : 스펙트럼 CT를 이용한 요오드 정량화의 정확성과 화학 색전술의 영상화 바이오 마커로서 요오드화 기름 침착 정량 분석의 잠재력을 평가하고자 한다.

재료 및 방법 : 서로 다른 양의 요오드화 기름 (0 - 8 vol%)을 포함하는 6 개의 인공 종양이 있는 간 팬텀을 만들었다. 이를 스펙트럼 CT로 촬영하여 요오드화 기름 밀도 (mg/mL) 및 Hounsfield unit (HU) 값을 측정하였다. 또한, 23 마리의 토끼에 VX2 간종을 이식하였다. 요오드화 기름-항암제 혼합물을 사용한 화학 색전술 후, 토끼를 스펙트럼 CT로 촬영하였다. 종양 내 요오드화 기름의 침착을 요오드화 기름의 밀도 및 HU로 정량화하였고, 병리학적 완전 반응의 예측은 receiver operating characteristic 곡선 분석으로 평가되었다.

결과 : 실제 요오드 밀도와 스펙트럼 이미지 기반 측정의 평균 차이는 0.5 mg/mL였다. 평균 HU는 평균 요오드 밀도 (r^2 = 1.000, p <.001)와 높은 상관관계가 있었다. 동물 연구에서 23마리 토끼 중 17마리 (73.9 %)에서 병리학적 완전 반응을 보였다. 요오드와 HU 측정 값의 곡선 아래 면적은 .863에서 .882 사이였다. 종양의 요오드화 기름의 0.7 vol%에 해당하는 3.57 mg/mL의 요오드 밀도는 70.6 %의 민감도와 100.0 %의 특이도를 가진 병리학적 완전 반응을 예측했다.

결론 : 스펙트럼 CT 영상은 표적의 요오드화 기름을 정량적으로 평가하여 화학 색전술 후 종양 반응을 예측할 수 있는 잠재력을 가지고 있다.

.....

주요어 : 경동맥 화학색전술, 간암, 스펙트럼 CT, 요오드화 기름, 정량화

학 번 : 2015-22008